IEEE Access
Multidisciplinary | Rapid Review | Open Access Journal

Received March 20, 2019, accepted April 7, 2019, date of publication April 18, 2019, date of current version April 29, 2019.

Digital Object Identifier 10.1109/ACCESS.2019.2911712

Numerical Study on Natural Convective Heat Transfer of Nanofluids in Disc-Type Transformer Windings

YUNPENG ZHANG, SIU-LAU HO, WEINONG FU, XINSHENG YANG, AND HUIHUAN WU
Department of Electrical Engineering, The Hong Kong Polytechnic University, Hong Kong

Corresponding author: Weinong Fu (eewnfu@polyu.edu.hk)

This work was supported by the Research Grant Council of the Hong Kong SAR Government under Project PolyU 152118/15E and Project G-YBY7.

ABSTRACT Nanofluid is an innovative approach to improve the thermal conductivity of fluid by adding nanoparticles. Transformer oil-based nanofluids have been prepared and measured, which verifies the concept and demonstrates the potential in oil-immersed power transformer applications. In this paper, the effect that nanofluids (oil/SiC) have on the natural convective heat transfer in disc-type transformer windings is investigated numerically. The multi-phase mixture model is employed for the first time to analyze such a nanofluid flow field, and the single-phase model is also used for comparison and mutual authentication. After using the nanofluid, significant temperature drops inside the windings are observed, and in some cases, the heat transfer performance is further improved by the adjusted mass flow rate distribution. The impact of nanofluids is enhanced with the rising volume fraction of nanoparticles. Before performing the study, the numerical model is validated using the existing results of the referenced windings cooled by transformer oil.

INDEX TERMS Disc-type winding, fluid flow, nanofluid, numerical simulation, power transformer, thermal management.

I. INTRODUCTION

Mineral oil has been widely used in power transformers to serve as the coolant and the dielectric, especially for high-voltage and high-power transformers. According to the cooling mechanism, oil-immersed transformers can be classified either as natural oil cooling (ON), oil forced cooling (OF), or oil directed cooling (OD). ON transformers have a simple structure and high stability. The lift force of flow is generated by the density discrepancy of oil at different temperatures. OF transformers acquire an improvement on the convection coefficients of cooling equipment by increasing the velocity of flow with the help of pumps, while the oil flow in the windings is still a thermosiphon flow. To reduce the hot-spot temperature, oil is pumped and forced to flow through the horizontal cooling ducts in the windings, and this type of transformer is named OD transformer. However, the increase in flow velocity exacerbates the electrification of oil. The accumulated charges may discharge onto the insulation board and shorten the transformer service life [1]. Another approach to enhance the heat transfer performance of oil-immersed transformers is to improve the inherently low thermal conductivity of transformer oil by dispersing solid particles of high thermal conductivity into the oil. This concept was proposed by Maxwell and realized by Eastman *et al.* [2] for the first time using nanoparticles. The mixture, prepared with base fluids and nanoparticles, is named nanofluid. Properties of transformer oil-based nanofluids with different nanoparticles and concentrations have been measured, which show significant improvement in terms of thermal conductivity [3]–[5]. The DC/AC dielectric strength of transformer oil-based nanofluids with specific nanoparticles and volume fractions is enhanced simultaneously [4]–[6].

Accurate prediction of the hot-spot temperature-rise in transformer windings is crucial for an appropriate thermal design. The thermal-hydraulic networks are proposed to determine the temperature and the flow distribution

The associate editor coordinating the review of this manuscript and approving it for publication was Fuhui Zhou.

in oil-immersed transformer windings, in which the heat conduction sub-model and the hydraulic sub-model are coupled by the boundary conditions on the solid-liquid interfaces [7], [8]. Numerical methods, which have the ability to handle irregular geometry, complex flow field and material nonlinearity, have also been applied in the thermal performance analysis of oil-immersed transformer windings [9]–[14]. In order to evaluate the hot-spot temperature-rise of windings accurately, both solid parts and coolants are considered in the computational domain. This is especially critical for ON transformers, in which the heat transfer is strongly coupled with the oil flow [15]. In numerical methods, such as finite volume method (FVM), the heat transfer between windings and coolants are solved without any boundary conditions imposed on the interface. Temperature-dependent parameters, such as material properties and boundary conditions, are readily embedded in the numerical model [12]. In a word, more detailed and accurate solutions could be derived using numerical methods.

According to the literatures [3], [4], [6], several categories of transformer oil-based nanofluids have been prepared and measured. However, there is no numerical analysis or experimental study on the temperature and flow distribution in nanofluid cooled transformer windings. In the literatures [16]–[19], which numerically analyze the nanofluid flow in simple containers, two types of models are used to characterize the nanofluid, and they are, namely, the single-phase model and the multi-phase model. As nanofluid consists of two phases, the solid phase and the liquid phase, the use of multi-phase model is straightforward, and multi-phase models, such as the mixture model and the Eulerian model, are reported to be more precise than the single-phase model [17]–[19]. In the single-phase model, the nanofluid is regarded as a homogenous mixture with equivalent properties [20], [21]. In the multi-phase models, interactions between phases are considered, and the volume fraction distribution of phases can be derived along with the fields. The major drawback of multi-phase models is more equations are involved in the governing equations.

In this paper, the disc-type windings of a natural nanofluid (oil/SiC) cooling transformer are modelled and analyzed numerically. It is the first time to implement the mixture model to study such a nanofluid flow field, and the single-phase model is also used for comparison and mutual authentication. The existing results of the referenced windings cooled by transformer oil [9] are treated as the references for the validation of the numerical model. The evaluation focuses on the changes in temperature profile, mass flow rate distribution and pressure drop after using the nanofluid. In order to give a rounded analysis, the effect of volume fraction of nanoparticles is taken into consideration.

II. MATHEMATICAL MODELLING

Owing to the axisymmetric structure of the windings, two–dimensional (2D) model [22] instead of three–dimensional (3D) model [10] is employed in the following analysis. The governing equations used to represent the fields depend on the pattern of fluid motion and the nanofluid model. In the single-phase model, the nanofluid is regarded as conventional single-phase fluid. Nanofluid is modelled integrally using the equivalent properties, and no more additional terms or equations are required for the dispersed nanoparticles. These multi-phase models, such as the mixture model, take these terms and equations into account. Moreover, the nanofluid flow in the ON transformer windings is laminar, since the velocities are quite low. Hence no turbulence model is needed. The problem of continuous fields is then discretized and solved with numerical methods and the mesh file of the computational domain. In this paper, the FVM based software package Ansys-FLUENT is adopted to solve the convective heat transfer problem.

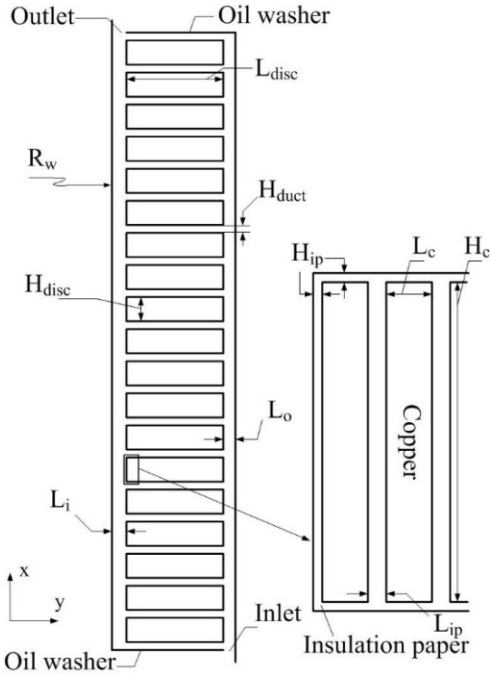

FIGURE 1. The configuration of one pass of the low-voltage windings.

A. GEOMETRY AND BOUNDARY CONDITIONS

The low-voltage windings of an ON power transformer rated at 66MVA [9], in which the regular transformer oil is replaced by nanofluid (oil/SiC), are modified and modelled to evaluate the performance of nanofluid. An axisymmetric 2D model is built for one pass of the low-voltage windings, as shown in Fig. 1. This pass contains two vertical ducts, twenty horizontal ducts and nineteen discs, and the horizontal ducts and the discs are sequentially numbered according to the X-axis direction, respectively. The insulation paper around the conductors is also taken into consideration in the model. The notations in Fig. 1 have the following dimensions:

$$L_{disc} = 0.0522(m)$$
$$R_w = 0.3162(m)$$

$$
\begin{aligned}
H_{duct} &= 0.0051(m)\\
H_{disc} &= 0.015(m)\\
L_o &= 0.0064(m)\\
L_i &= 0.0089(m)\\
H_{ip} &= 0.0004(m)\\
L_{ip} &= 0.0008(m)\\
L_c &= 0.0021(m)\\
H_c &= 0.0143(m)
\end{aligned}
$$

As Fig. 1 shows, oil flows into this pass from the outer vertical duct, through the horizontal ducts and out of this pass from the inner vertical duct. The oil that flows in the horizontal ducts of the subsequent pass is exactly in the opposite direction of that in this pass. These two types of passes with opposite inlet positions constitute the zig-zag cooling system of windings. Therefore, the pass with inlet on the inner vertical duct is also included in the following analysis.

The conductors are imposed on homogeneous heat sources ($676.9W/disc$), which are conducted to the solid-liquid interface and dissipated to the coolants through convection. These two oil washers and the surrounding cylinders with low thermal conductivity are considered as adiabatic. The inlet boundary condition derived by heat run test is an isothermal flow ($T_{inlet} = 319.85K$) with the velocity of $0.0592\ m/s$, and the outlet is set with a pressure boundary condition ($0\ Pa$). This inlet boundary condition applies to the transformer oil cooling and the nanofluid cooling, and the influence of nanofluid on the inlet flow is neglected to isolate the effect that nanofluid has on the convective heat transfer inside the windings.

TABLE 1. Material properties.

Material	Density ($kg\ m^{-3}$)	Specific heat ($W\ kg^{-1}\ K^{-1}$)	Thermal conductivity ($W\ m^{-1}\ K^{-1}$)
Copper	8933	385	401
Insulation	930	1340	0.19
SiC	3160	750	490

B. MATERIAL PROPERTIES

The properties of SiC nanoparticle with the diameter of $100nm$ are listed in Table 1 along with the properties of copper and insulation paper. All these properties are considered as temperature independent, while the properties of transformer oil vary with temperature as follows [12]:

$$\rho_f = 1098.72 - 0.712T \quad (1)$$

$$C_f = 807.163 + 3.58T \quad (2)$$

$$\mu_f = 0.08467 - 4.0\times10^{-4}T + 5.0\times10^{-7}T^2 \quad (3)$$

$$k_f = 0.1509 - 7.101\times10^{-5}T \quad (4)$$

where; ρ, C, μ, and k are density, specific heat, viscosity and thermal conductivity, respectively; the transformer oil is indexed by the subscript f.

C. THE SINGLE-PHASE MODEL

In the single-phase model of nanofluid [16]–[21], it is assumed that the nanoparticles are uniformly dispersed in the base fluid. Moreover, the velocity discrepancy and interactions between phases are neglected. The properties of nanofluid are represented by equivalent models which are affected by multiple variables, such as the species, the dimension and the volume fraction of nanoparticles. The formulas for the density and the specific heat of nanofluid is relatively straightforward, as given by

$$\rho_{nf} = (1-\emptyset)\,\rho_f + \emptyset\rho_p \quad (5)$$

$$C_{nf}\,\rho_{nf} = (1-\emptyset)\,C_f\,\rho_f + \emptyset C_p\rho_p \quad (6)$$

where; $\emptyset$ is the volume fraction of nanoparticles; the nanofluid and the nanoparticle are noted by the subscript nf and p, respectively. However, for the viscosity and the thermal conductivity, a uniform model working for all types of nanofluids does not exist. In this paper, the Einstein viscosity formula based model [23] which considers the dimension of the nanoparticle is used to predict the nanofluid viscosity and the thermal conductivity model [24] derived by fitting experimental data is adopted

$$\mu_{nf} = \mu_f\left[1 + 2.5\emptyset\left(1 + \frac{8.868}{r}\right)\right] \quad (7)$$

$$k_{nf} = k_f\left[1 + 4.4Re_p^{0.4}Pr_f^{0.66}\left(\frac{T}{T_{fr}}\right)^{10}\left(\frac{k_p}{k_f}\right)^{0.03}\emptyset^{0.66}\right] \quad (8)$$

where; r is the average radius of the nanoparticle; Pr is the Prandtl number; T_{fr} is the freezing point of the base liquid; the Reynolds number of nanoparticle is defined as

$$Re_p = \frac{2\rho_f k_b T}{\pi\mu_f^2 d_p} \quad (9)$$

where; k_b is the Boltzmann constant ($1.38066\times10^{-23}JK^{-1}$); d_p is the diameter of the nanoparticle. It is worth noting that the viscosity and the thermal conductivity of nanofluids increase with the rising volume fraction. It can be seen from (8) and (9) that the influence of temperature on the thermal conductivity is considered in the model, while the interaction between phases is assumed to be temperature independent in other three models.

The Reynolds number for the nanofluid flow in the windings is calculated to determine the flow pattern. The average velocity is replaced by the inlet velocity which is relatively large, and the calculated Reynolds numbers (<1000) for all the flows in this study are much smaller than the critical Reynolds number of turbulence (2100). Therefore, the studied nanofluid flows are all laminar. The governing equations for laminar nanofluid flow represented by the single-phase model are identical to that of conventional single-phase flow, as given by

Continuity,

$$\nabla\cdot\left(\rho_{nf}\boldsymbol{V}\right) = 0 \quad (10)$$

Momentum and,

$$\nabla \cdot \left(\rho_{nf} \boldsymbol{V}\boldsymbol{V}\right) = -\nabla P + \nabla \cdot \left(\mu_{nf} \nabla \boldsymbol{V}\right) + \rho_{nf} \boldsymbol{g} \tag{11}$$

Energy,

$$\nabla \cdot \left(\rho_{nf} \boldsymbol{V} C_{nf} T\right) = \nabla \cdot \left(k_{nf} \nabla T\right) + S_e \tag{12}$$

where; $\boldsymbol{V}$ is the velocity vector; P is the pressure; $\boldsymbol{g}$ is the gravity vector; S_e is the heat source.

D. THE MIXTURE MODEL

Like the single-phase model, the governing equations of continuity, momentum and energy in the mixture model are formulated for the mixture rather than for each phase, while the velocity difference and the interaction between phases are considered in the momentum and energy equations [18], [19]. Moreover, one more equation for the volume fraction of nanoparticles is included in the governing equations, which are given by

Continuity,

$$\nabla \cdot \left(\rho_{nf} \boldsymbol{V_m}\right) = 0 \tag{13}$$

Momentum,

$$\nabla \cdot \left(\rho_{nf} \boldsymbol{V_m} \boldsymbol{V_m}\right) = -\nabla P + \nabla \cdot \tau + \rho_{nf} \boldsymbol{g} + \nabla \cdot \left(\sum_{k=1}^{2} \emptyset_k \rho_k \boldsymbol{V}_{dr,k} \boldsymbol{V}_{dr,k}\right) \tag{14}$$

Energy and,

$$\nabla \cdot \left(\sum_{k=1}^{2} \emptyset_k \boldsymbol{V}_k \left(\rho_k E_k + P\right)\right) = \nabla \cdot \left(k_{nf} \nabla T\right) + S_e \tag{15}$$

Volume fraction,

$$\nabla \cdot \left(\emptyset \rho_p \boldsymbol{V}_m\right) = \nabla \cdot \left(\emptyset \rho_p \boldsymbol{V}_{dr,p}\right) \tag{16}$$

$\boldsymbol{V}_m$ is the mass-averaged velocity of the nanofluid

$$\boldsymbol{V}_m = \frac{\sum_{k=1}^{2} \emptyset_k \rho_k \boldsymbol{V}_k}{\rho_{nf}} \tag{17}$$

The stress tensor τ is defined as:

$$\tau = \mu_{nf} \nabla \boldsymbol{V}_m \tag{18}$$

The drift velocity $\boldsymbol{V}_{dr,p}$ is connected to the relative velocity $\boldsymbol{V}_{pf}$ by the following formula:

$$\boldsymbol{V}_{dr,p} = \boldsymbol{V}_{pf} - \sum_{k=1}^{2} \frac{\emptyset_k \rho_k}{\rho_{nf}} \boldsymbol{V}_{fk} \tag{19}$$

An algebraic formulation for the relative velocity [25], which is based on the assumption of a local equilibrium between phases over a short length scale, is adopted

$$\boldsymbol{V}_{pf} = \frac{\rho_p d_p^2}{18 \mu_f f_{drag}} \frac{\left(\rho_p - \rho_{eff}\right)}{\rho_p} \boldsymbol{a} \tag{20}$$

where $\boldsymbol{a}$ is the acceleration,

$$\boldsymbol{a} = \boldsymbol{g} - \left(\boldsymbol{V}_m \cdot \nabla\right) \boldsymbol{V}_m \tag{21}$$

and the drag force function f_{drag} is proposed by [26]

$$f_{drag} = \begin{cases} 1 + 0.15 Re_p^{0.687} & Re_p \leq 1000 \\ 0.0183 Re_p & Re_p > 1000 \end{cases} \tag{22}$$

In the mixture model, the governing equations, which include the continuity equation of the mixture, the momentum equation of the mixture, the energy equation of the mixture, the volume fraction equation of the secondary phase, and the algebraic expressions of the relative velocities, are solved. As a consequence, the number of variables in the mixture model is larger than the single-phase model and smaller than the full multiphase model.

III. RESULTS AND DISCUSSION

A. MODEL VALIDATION AND GRID-INDEPENDENCE STUDY

Both the transformer oil flow and the nanofluid flow are solved with the pressure-based steady-state solver in a coupled manner. To validate the accuracy of the numerical model and the solver, the referenced wingding [9] is recalculated firstly, solutions of which are compared with the existing results in [9]. As shown in Fig. 2(a), the same hot-spot location (disc 16) with the temperature of 365.04K is derived, and the error of this maximum temperature is about 0.9% (3.5K). In addition, the results of mass flow rate fraction obtained in this paper, which are given in Fig. 2(b), are in good agreement with those given in [9]. Consistent with the reference, the first duct has the largest mass flow rate fraction, which is located in the interval (18%, 19%), and the mass flow rate fraction of the last duct is relatively small, about 3%. Hence the correctness of the numerical model and the solver is validated.

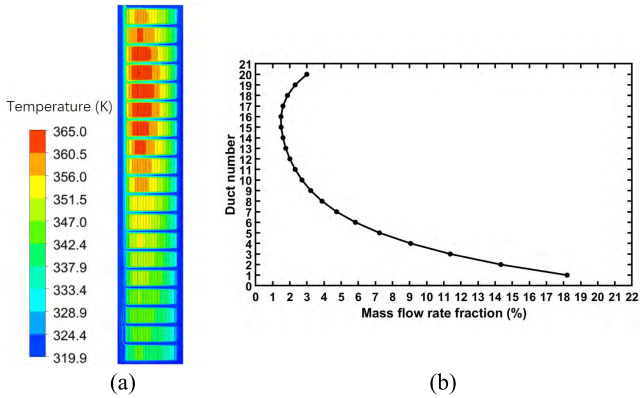

FIGURE 2. (a) The temperature contours and (b) the flow distribution of the referenced winding.

These two modified passes with transformer oil cooling are solved with the validated solver, and the results are treated as the references for the nanofluid cooling to estimate the heat transfer performance. The contours of the temperature of these two passes with opposite inlet positions are given in Fig. 3. With more coolant flowing into the later pass shown in Fig. 3(b), its hot-spot temperature is much lower than that of the former pass. There are approximately 1.2 million

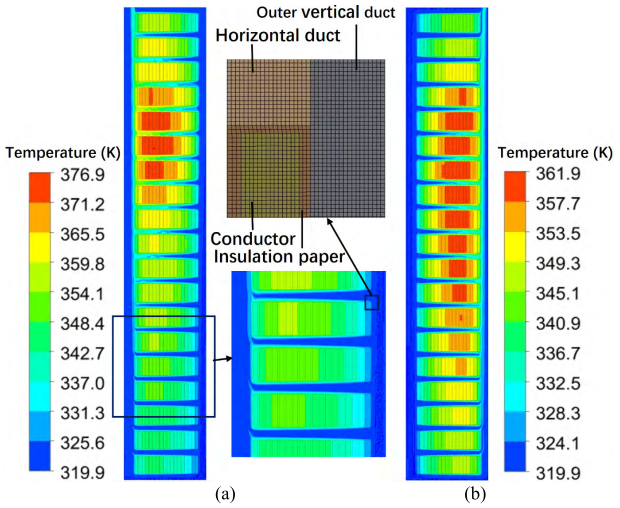

FIGURE 3. (a) Contours of the temperature of the pass with inlet on the outer vertical duct and part of the generated mesh. (b) Contours of the temperature of the pass with inlet on the inner vertical duct.

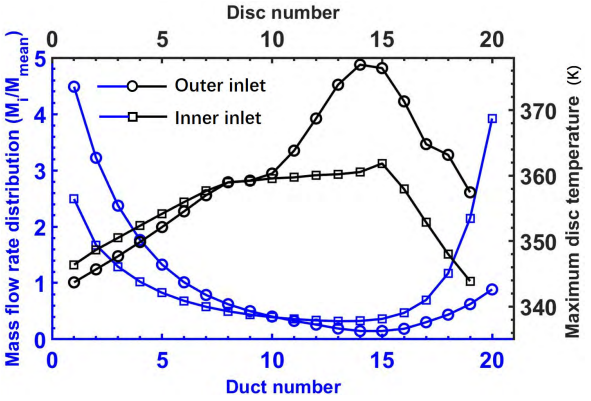

FIGURE 4. Flow and temperature distribution for passes with inlet on the inner and outer vertical ducts.

quadrilateral elements in the FVM mesh, part of which is shown in Fig. 3(a). The mass flow rate distribution in the horizontal ducts is obtained and shown in Fig. 4. It is worth noting that the pass with inlet on the inner vertical duct has a relatively uniform mass flow rate distribution, leading to a smaller temperature discrepancy among the discs. Discs surrounded by ducts with the smallest mass flow rate distribution (*MFRD*), which is defined as

$$MFRD_i = \frac{M_i}{\left(\sum_{k=1}^{20} M_k\right)/20} = \frac{M_i}{M_{mean}} \tag{23}$$

rather than the top discs, have the highest temperature-rise (see Fig. 4). The hot-spot locations of these two passes are disc fourteen and disc fifteen, respectively.

Mesh generated in the analysis of transformer oil cooling is used in the study of oil/SiC nanofluid (1% volume fraction of nanoparticles) cooling, and refined meshes with more elements are introduced to ensure the grid-independence of the results. For flows in simple geometries, a general reference for the grid-independence is the variation in the average Nusselt number [27]. Since the pass geometry is complicated, it is difficult to determine the characteristic length, the heat flux and the temperature difference for the whole system. Another alternative for grid-independence validation is to compare the maximum and mean temperature variation [9]. Two refined meshes with about 8% and 16% more elements are generated by constraining the element sizing globally. The maximum temperature and average temperature changes are less than 0.2% (0.59K) and 0.3% (0.97K) when using the single-phase model, and the corresponding changes for the mixture model are 0.4% (1.39K) and 0.3% (0.85K), respectively. Then the initial mesh is feasible for this specific problem.

B. COMPARISON BETWEEN THE NANOFLUID COOLING AND THE TRANSFORMER OIL COOLING

For a convection flow, the heat transfer coefficient on the solid-liquid interface increases with the improvement of the thermal conductivity of coolants. Hence the same amount of heat could be dissipated to the ambient coolants with a relatively small temperature difference. In addition to the thermal conductivity, the viscosity of transformer oil is increased by adding nanoparticles. In the following analysis, the transformer oil is replaced by the oil/SiC nanofluid (1% volume fraction of nanoparticles), and the numerical results of transformer oil cooling are used as the references for nanofluid cooling.

The mixture model is implemented to study the nanofluid flow in the windings, and the single-phase model is also used for comparison and mutual authentication. The pass with inlet on the outer vertical duct is calculated firstly, and an overall reduction in temperature is observed through comparing the results with the references, as shown in Fig. 5(a) and Fig. 6(b). The maximum temperature-rise reduction in Fig. 5(a), which is calculated for each disc, is defined as follows:

$$p_1 = T_f^{max} - T_{nf}^{max} \tag{24}$$

It can be found that the peak locations in Fig. 5(a) are almost coincident with the peak location of the transformer oil cooling temperature profile, which is shown in Fig. 4. The results of relative mass flow rate increment, which is calculated for each duct and defined by

$$p_2 = \frac{MFRD_{nf} - MFRD_f}{MFRD_f} \tag{25}$$

explain and confirm the variation on maximum temperature-rise of each disc (see Fig. 5(b)). Moreover, the heat transfer coefficient of disc is increased in a similar manner to the curve given in Fig. 5(a). It is worth noting that these two models give quite close results for the thermal and fluidic field in the windings, which strengthens the effectiveness of the numerical analysis by mutual authentication.

The detailed results of the mass flow rate distribution of this pass are listed in Table 2 for a clear illustration. The superscripts P, S, and M represent the solution of the pure transformer oil, the single-phase model, and the mixture model.

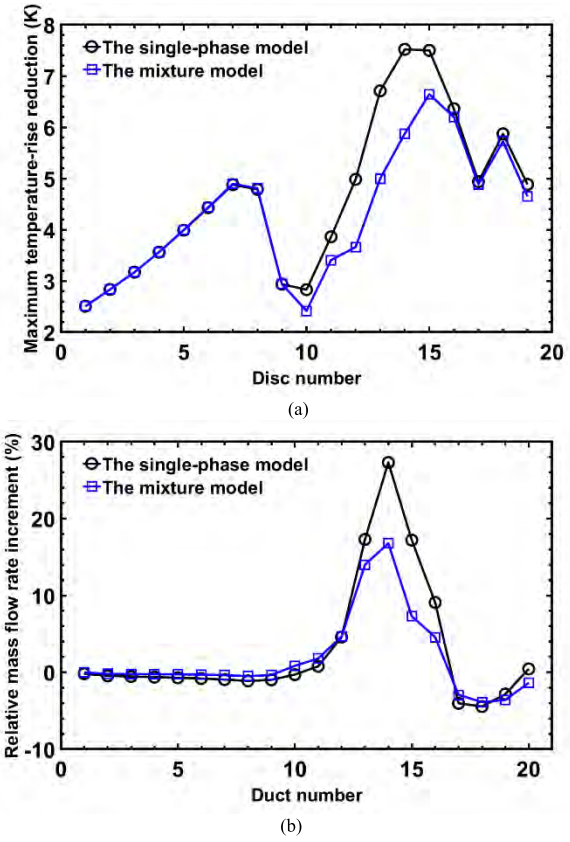

FIGURE 5. (a) Maximum temperature-rise reduction and (b) relative mass flow rate increment for the pass with inlet on the outer vertical duct and nanofluid cooling.

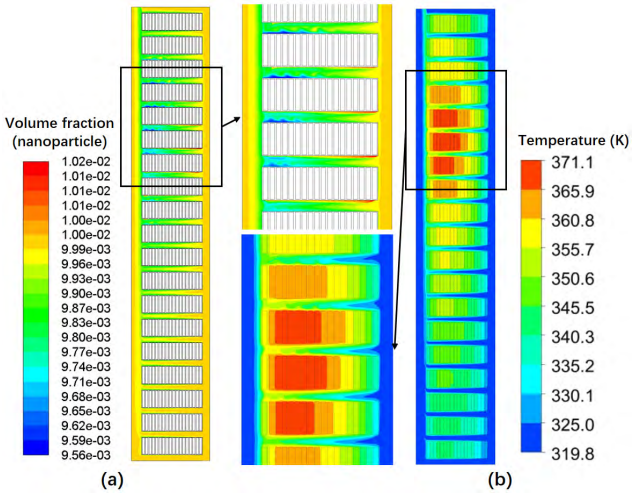

FIGURE 6. (a) Distribution of the volume fraction of nanoparticles and (b) contours of the temperature derived by the mixture model for the pass with inlet on the outer vertical duct and nanofluid cooling.

Compared with the mixture model, larger *MFRD* increments are derived by the single-phase model in the ducts 13, 14, 15, and 16, which have the smallest *MFRD*.

Thus, a better performance is obtained in the vicinity of the hot-spot disc using the single-phase model, by virtue

TABLE 2. Mass flow rate distribution.

Duct	$MFRD^P$	$MFRD^S$	$MFRD^M$	$p_2{}^S$	$p_2{}^M$
1	4.486	4.478	4.485	-0.18%	-0.03%
2	3.223	3.208	3.216	-0.45%	-0.20%
3	2.373	2.360	2.367	-0.55%	-0.23%
4	1.763	1.752	1.758	-0.62%	-0.25%
5	1.326	1.316	1.322	-0.71%	-0.26%
6	1.012	1.004	1.009	-0.81%	-0.30%
7	0.787	0.779	0.784	-0.95%	-0.37%
8	0.622	0.616	0.619	-1.12%	-0.50%
9	0.499	0.495	0.498	-0.98%	-0.36%
10	0.403	0.402	0.407	-0.30%	0.84%
11	0.327	0.329	0.332	0.79%	1.80%
12	0.261	0.273	0.273	4.59%	4.65%
13	0.191	0.224	0.218	17.28%	13.96%
14	0.147	0.187	0.172	27.34%	16.84%
15	0.147	0.172	0.158	17.19%	7.29%
16	0.186	0.203	0.195	9.09%	4.56%
17	0.303	0.290	0.294	-4.03%	-2.93%
18	0.437	0.417	0.420	-4.45%	-3.88%
19	0.623	0.606	0.601	-2.83%	-3.59%
20	0.885	0.889	0.873	0.44%	-1.37%
Sum	20.000	20.000	20.000		

of the higher relative mass flow rate increment as shown in Fig. 5(b). There is a maximum difference of 1.7% in the heat transfer coefficient of disc between these two models. Owing to the great density of dispersed nanoparticles, the density of nanofluid is higher than that of transformer oil. The velocity of flow, which is another variable involved in the drag equation, decreases slightly after the addition of nanoparticles. Under the combined effect of increasing density and decreasing velocity, the pressure drop in this pass, which is defined as the difference between the mass flow averaged pressures at the inlet and outlet, is reduced slightly when using this nanofluid, as shown in Fig. 7.

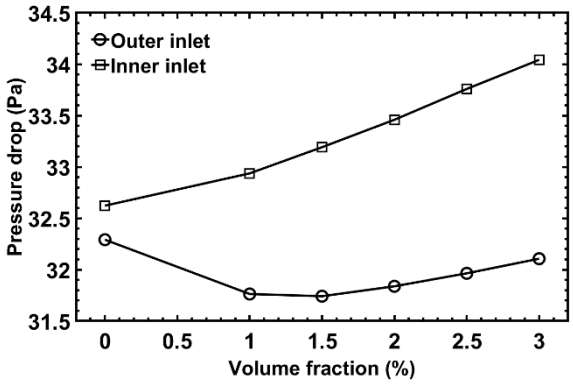

FIGURE 7. Pressure drop as a function of volume fraction.

As introduced before, the equation for the volume fraction of nanoparticles is included in the mixture model, and the results for the pass with inlet on the outer vertical duct is

shown in Fig. 6(a). Overall, the concentration of nanoparticle is inversely proportional to the temperature of nanofluid. For nanofluid in the horizontal ducts, the inside temperature is much higher than the outside temperature. Hence these horizontal ducts witness an upward trend in the volume fraction from the inside of ducts to the outside of ducts, which is opposite to the trend in temperature change.

The nanofluid flow in the pass with inlet on the inner vertical duct is calculated and compared to the reference. It is found that the influence of nanofluid on the mass flow rate distribution is relatively small, as shown in Fig. 8(b). Even so, a more pronounced effect is derived with the single-phase model. The improvement on heat transfer is mainly achieved by the increased thermal conductivity, hence the thermal field results obtained by these two models, which are given in Fig. 8(a), are roughly consistent. Comparing the results of these two models, the maximum difference in the heat transfer coefficient of disc is less than 0.2%. With a weak effect on the flow field and a significant increase in the density, the pressure drop in this pass increases slightly after using the nanofluid, as shown in Fig. 7.

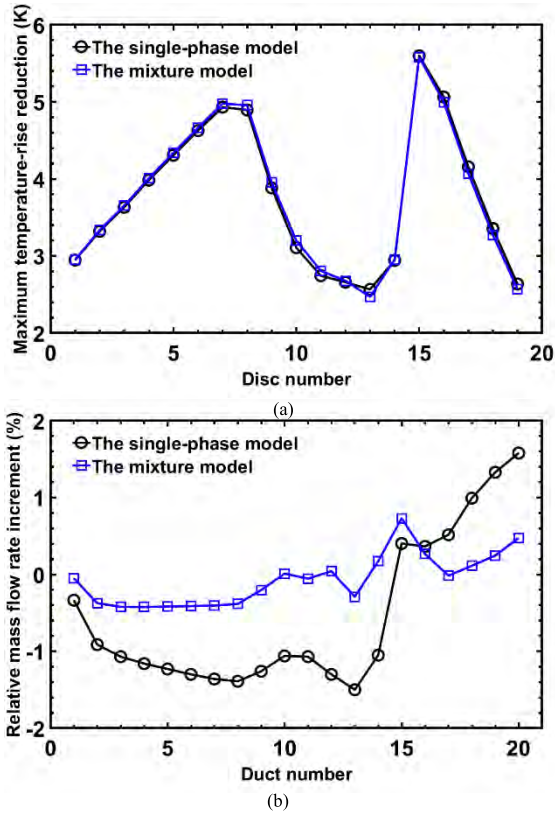

FIGURE 8. (a) Maximum temperature-rise reduction and (b) relative mass flow rate increment for the pass with inlet on the inner vertical duct and nanofluid cooling.

Despite the varying effects that nanofluids have on the flow fields, the improvement in thermal conductivity produces distinct temperature drops over the entire pass. Moreover, it is concluded from the results of these two passes that the heat transfer performance can be further improved by the adjusted mass flow rate distribution. The effectiveness of the numerical analysis is strengthened by the mutual authentication of these two models. Since the mixture model is reported to be more precise than the single-phase model [18], [19], the mixture model is adopted in the following analysis of volume fraction.

C. EFFECT OF THE VOLUME FRACTION

The impact that the volume fraction of nanoparticles has on the heat transfer in the windings is measured by considering four more nanofluids with the volume fraction of 1.5%, 2%, 2.5%, and 3%. The calculated results for these two passes are given in Fig. 9 and Fig. 10, respectively. The numerical results obtained in the former section are also included in these figures for comparison. It is worth noting that the overall tendency of these two parameters (p_1 and p_2) along the flow direction is maintained, while the effect of nanofluid is enhanced with the rising volume fraction. Hence there is a positive correlation between the volume fraction and the heat transfer performance. However, the pressure drops in these two passes grow as well, as shown in Fig. 7, especially for the pass with inlet on the inner vertical duct. More powerful pumps are required to compensate the increasing pressure

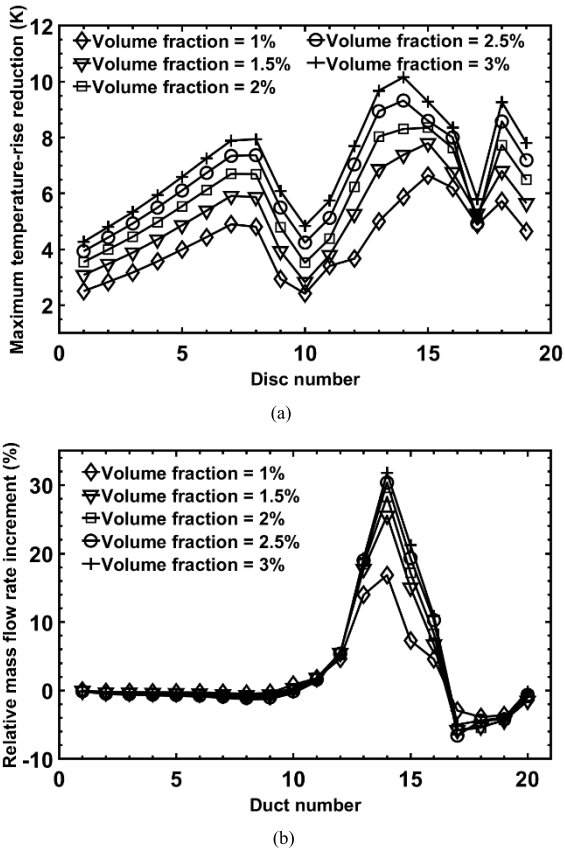

FIGURE 9. (a) Maximum temperature-rise reduction and (b) relative mass flow rate increment as a function of volume fraction for the pass with inlet on the outer vertical duct.

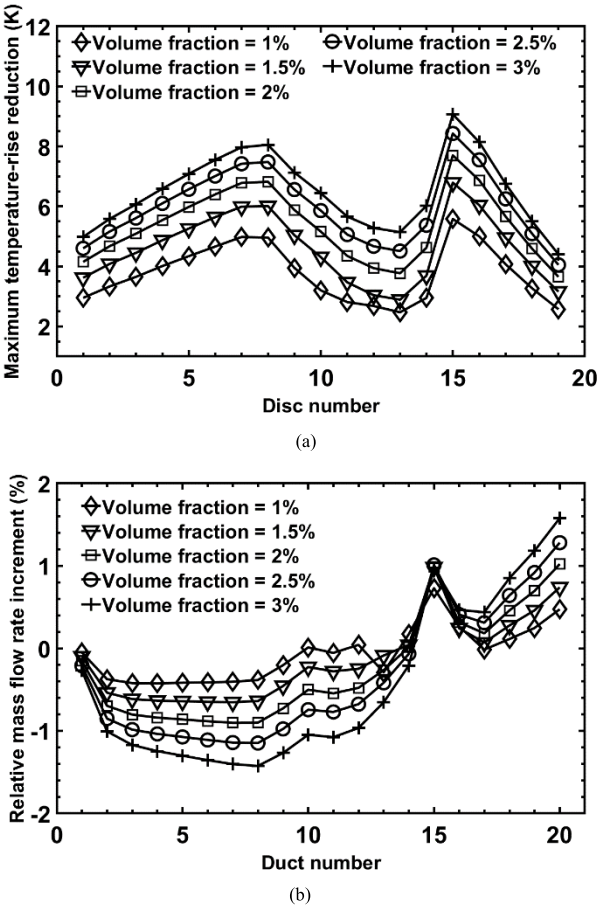

FIGURE 10. (a) Maximum temperature-rise reduction and (b) relative mass flow rate increment as a function of volume fraction for the pass with inlet on the inner vertical duct.

drop across the windings. All these observed variations are correlated with the properties of nanofluids, which are determined by the volume fraction of the nanoparticles. To cope with these mentioned factors and the cost, optimization algorithms may be used to find the Pareto front for practical application, and the flexibility of nanofluids makes it possible to prepare the coolants as required.

IV. CONCLUSION

In this paper, the heat transfer in disc-type transformer windings cooled by natural oil/SiC nanofluid is investigated numerically. Although nanofluids have different effects on the flow fields, distinct temperature drops can be observed in these two passes after using the nanofluid. The pass with inlet on the outer vertical duct also witnesses a significant improvement in the mass flow rate distribution, which further improves the heat transfer performance of the nanofluid. Both the mixture model and the single-phase model are adopted in the analysis, and the effectiveness of the numerical analysis is strengthened by the mutual authentication of these two models. When increasing the volume fraction of nanoparticles, the nanofluids produce enhanced effects on the heat transfer and the flow field, which is accompanied by an increase in the pressure drop.

REFERENCES

[1] R. M. Radwan, R. M. El-Dewieny, and I. A. Metwally, "Investigation of static electrification phenomenon due to transformer oil flow in electric power apparatus," *IEEE Trans. Electr. Insul.*, vol. 27, no. 2, pp. 278–286, Apr. 1992.

[2] J. A. Eastman, S. U. S. Choi, S. Li, W. Yu, and L. J. Thompson, "Anomalously increased effective thermal conductivities of ethylene glycol-based nanofluids containing copper nanoparticles," *Appl. Phys. Lett.*, vol. 78, no. 6, pp. 718–720, Feb. 2001.

[3] C. Choi, H. S. Yoo, and J. M. Oh, "Preparation and heat transfer properties of nanoparticle-in-transformer oil dispersions as advanced energy-efficient coolants," *Current Appl. Phys.*, vol. 8, no. 6, pp. 710–712, Oct. 2008.

[4] S. C. Pugazhendhi, "Experimental evaluation on dielectric and thermal characteristics of nano filler added transformer oil," in *Proc. ICHVE*, Shanghai, China, Sep. 2012, pp. 207–210.

[5] D. Liu, Y. Zhou, Y. Yang, L. Zhang, and F. Jin, "Characterization of high performance AIN nanoparticle-based transformer oil nanofluids," *IEEE Trans. Dielectr. Electr. Insul.*, vol. 23, no. 5, pp. 2757–2767, Oct. 2016.

[6] Y. Lv, M. Rafiq, C. Li, and B. Shan, "Study of dielectric breakdown performance of transformer oil based magnetic nanofluids," *Energies*, vol. 10, no. 7, p. 1025, Jul. 2017.

[7] J. Zhang and X. Li, "Oil cooling for disk-type transformer windings —Part 1: Theory and model development," *IEEE Trans. Power Del.*, vol. 21, no. 3, pp. 1318–1325, Jul. 2006.

[8] J. Zhang and X. Li, "Oil cooling for disk-type transformer windings—Part II: Parametric studies of design parameters," *IEEE Trans. Power Del.*, vol. 21, no. 3, pp. 1326–1332, Jul. 2006.

[9] F. Torriano, M. Chaaban, and P. Picher, "Numerical study of parameters affecting the temperature distribution in a disc-type transformer winding," *Appl. Therm. Eng.*, vol. 30, nos. 14–15, pp. 2034–2044, Oct. 2010.

[10] F. Torriano, P. Picher, and M. Chaaban, "Numerical investigation of 3D flow and thermal effects in a disc-type transformer winding," *Appl. Therm. Eng.*, vol. 40, pp. 121–131, Jul. 2012.

[11] A. Skillen, A. Revell, H. Iacovides, and W. Wu, "Numerical prediction of local hot-spot phenomena in transformer windings," *Appl. Therm. Eng.*, vol. 36, pp. 96–105, Apr. 2012.

[12] N. El Wakil, N.-C. Chereches, and J. Padet, "Numerical study of heat transfer and fluid flow in a power transformer," *Int. J. Therm. Sci.*, vol. 45, no. 6, pp. 615–626, 2006.

[13] X. Zhang, Z. Wang, and Q. Liu, "Prediction of pressure drop and flow distribution in disc-type transformer windings in an OD cooling mode," *IEEE Trans. Power Del.*, vol. 32, no. 4, pp. 1655–1664, Aug. 2017.

[14] S. Tenbohlen, N. Schmidt, C. Breuer, S. Khandan, and R. Lebreton, "Investigation of thermal behavior of an oil-directed cooled transformer winding," *IEEE Trans. Power Del.*, vol. 33, no. 3, pp. 1091–1098, Jun. 2018.

[15] L. W. Pierce, "An investigation of the thermal performance of an oil filled transformer winding," *IEEE Trans. Power Del.*, vol. 7, no. 3, pp. 1347–1358, Jul. 1992.

[16] V. Bianco, F. Chiacchio, O. Manca, and S. Nardini, "Numerical investigation of nanofluids forced convection in circular tubes," *Appl. Therm. Eng.*, vol. 29, nos. 17–18, pp. 3632–3642, Dec. 2009.

[17] M. Kalteh, A. Abbassi, M. Saffar-Avval, A. Frijns, A. Darhuber, and J. Harting, "Experimental and numerical investigation of nanofluid forced convection inside a wide microchannel heat sink," *Appl. Therm. Eng.*, vol. 36, pp. 260–268, Apr. 2012.

[18] M. H. Fard, M. N. Esfahany, and M. R. Talaie, "Numerical study of convective heat transfer of nanofluids in a circular tube two-phase model versus single-phase model," *Int. J. Heat Mass Transf.*, vol. 37, no. 1, pp. 91–97, Jan. 2010.

[19] R. Lotfi, Y. Saboohi, and A. M. Rashidi, "Numerical study of forced convective heat transfer of nanofluids: Comparison of different approaches," *Int. J. Heat Mass Transf.*, vol. 37, no. 1, pp. 74–78, Jan. 2010.

[20] W. Rashmi, A. F. Ismail, M. Khalid, and Y. Faridah, "CFD studies on natural convection heat transfer of Al_2O_3-water nanofluids," *Heat Mass Transf.*, vol. 47, no. 10, pp. 1301–1310, Oct. 2011.

[21] H. F. Oztop and E. Abu-Nada, "Numerical study of natural convection in partially heated rectangular enclosures filled with nanofluids," *Int. J. Heat Fluid Flow*, vol. 29, no. 5, pp. 1326–1336, Oct. 2008.

[22] X. Zhang, Z. Wang, Q. Liu, P. Jarman, and M. Negro, "Numerical investigation of oil flow and temperature distributions for ON transformer windings," *Appl. Therm. Eng.*, vol. 130, pp. 1–9, Feb. 2018.
[23] P. Xiaofei, "Study of nanofluids heat transfer performance in high temperature condition based on vehicular cooler," Ph.D. dissertation, Dept. Elect. Eng., Zhejiang Univ., Zhejiang, China, 2007.
[24] M. Corcione, "Empirical correlating equations for predicting the effective thermal conductivity and dynamic viscosity of nanofluids," *Energy Convers. Manage.*, vol. 52, no. 1, pp. 789–793, Jan. 2011.
[25] M. Manninen, V. Taivassalo, and S. Kallio, "On the mixture model for multiphase flow," VTT Tech. Res. Centre Finland, Espoo, Finland, VTT Publications 288, 1996.
[26] L. Schiller and A. Naumann, "A drag coefficient correlation," *Z. Vereins Deutscher Ing.*, vol. 77, pp. 318–320, Jan. 1935.
[27] M. Kalteh, A. Abbassi, M. Saffar-Avval, and J. Harting, "Eulerian–Eulerian two-phase numerical simulation of nanofluid laminar forced convection in a microchannel," *Int. J. Heat Fluid Flow*, vol. 32, no. 1, pp. 107–116, Feb. 2011.

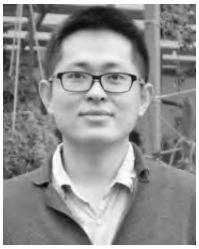

YUNPENG ZHANG received the B.Sc. degree in electrical engineering from Shandong University, Jinan, China, in 2011, and the M.Sc. degree in electrical engineering from The Hong Kong Polytechnic University, Hong Kong, in 2016, where he is currently pursuing the Ph.D. degree in electrical engineering.

His research interests include numerical methods of electromagnetic field computation, multi-physics simulation, and optimization design of transformers.

SIU-LAU HO received the B.Sc. and Ph.D. degrees in electrical engineering from The University of Warwick, Coventry, U.K., in 1976 and 1979, respectively.

He joined The Hong Kong Polytechnic University, Hung Hom, Hong Kong, in 1979, where he is currently a Chair Professor and an Associate Vice President. Since joining the university, he has been working actively with local industry, particularly in railway engineering. He is the holder of several patents and has authored over 250 conference papers and over 300 papers published in leading journals, mostly in the IEEE TRANSACTIONS and IET proceedings. His research interests include design optimization of electromagnetic devices, the application of finite elements in electrical machines, phantom loading of machines, and railway engineering.

Dr. Ho is a member of the Hong Kong Institution of Engineers.

WEINONG FU received the B.Eng. degree from the Hefei University of Technology, Hefei, China, in 1982, the M.Eng. degree from the Shanghai University of Technology, Shanghai, China, in 1989, and the Ph.D. degree from The Hong Kong Polytechnic University, Kowloon, Hong Kong, in 1999, all in electrical engineering.

He is currently a Professor with The Hong Kong Polytechnic University. Before joining the University in 2007, he was one of the key developers with Ansoft Corporation, Pittsburgh, PA, USA. He has about seven years of working experience with Ansoft, focusing on the development of the commercial software Maxwell. He has authored or coauthored 184 papers in refereed journals. His current research interests mainly include numerical methods of electromagnetic field computation, optimal design of electric devices based on numerical models, applied electromagnetics, and novel electric machines.

XINSHENG YANG received the B.Sc. and M.Sc. degrees in electrical engineering from the Hebei University of Technology, Tianjin, China, in 2010 and 2015, respectively, where he is currently pursuing the Ph.D. degree in electrical engineering.

From 2017 to 2019, he was a Research Assistant with The Hong Kong Polytechnic University, Kowloon, Hong Kong. His research interests include wireless power transmission and numerical methods of electromagnetic field computation.

HUIHUAN WU was born in Taiyuan, Shanxi, China, in 1990. He received the B.Sc. degree in automation from the Zhejiang University of Technology, in 2014, and the M.Sc. degree in electric engineering from The Hong Kong Polytechnic University, in 2016, where he is currently pursuing the Ph.D. degree in electrical engineering.

From 2016 to 2017, he was a Research Assistant with the Applied Electromagnetic Laboratory, The Hong Kong Polytechnic University. His research interests include design and optimization of high performance electric motor, topology optimization, and parallel computing.